This article has been accepted for publication in a future issue of this journal, but has not been fully edited. Content may change prior to final publication. Citation information: DOI 10.1109/JESTPE.2019.2894677, IEEE Journal of Emerging and Selected Topics in Power Electronics

Optimal Shaping of the MMC Circulating Currents for Preventing AC-side Power Oscillations from Propagating into HVDC Grids

Gilbert Bergna-Diaz, *Member IEEE*, Jon Are Suul, *Member IEEE*, Erik Berne, Jean-Claude Vannier, and Marta Molinas, *Member IEEE*

***Abstract*— A constrained optimization problem based on the Lagrange multipliers method is formulated to derive the circulating current references of Modular Multilevel Converters (MMC) directly in *abc* coordinates. The resulting analytic expressions for calculating the circulating current reference signals are designed to eliminate oscillations in the *dc*-side power flow, independently from the *ac*-side operation of the MMC. As a result of the constrained optimization, the circulating currents are shaped to optimally utilize the degrees of freedom provided by the internal energy buffering capacity of the MMC, to effectively decouple the *ac* grid conditions from the *dc* bus. This property of the proposed control method makes it especially suitable for preventing oscillations due to unbalanced *ac* grid voltage conditions from propagating into multi-terminal HVDC systems. It is shown that the power flow at the *dc*-side of the MMC will be most effectively decoupled from *ac*-side transients if the desired steady-state power flow is imposed by acting directly on the circulating current references instead of by acting on the *ac*-side current references. The operation of an MMC controlled by the proposed approach is demonstrated by simulation studies, verifying the ability of keeping the *dc* power flow free of second harmonic oscillations, independently of the power control objectives applied for calculating the *ac*-side current references of the converter.**

Index Terms— Circulating Current Control, Constrained Optimization, Energy Balancing Control, HVDC Transmission, Lagrange Multipliers Method, Modular Multilevel Converters.

Manuscript received February 28, 2018; revised August 15, 2018, October 31, 2018 and December 20, 2018; accepted December 22, 2018; date of current version, January 18, 2019 . The work of G. Bergna-Diaz was funded by the French Association of Research and Technology (ANRT) through a CIFRE PhD Fellowship. The work of SINTEF Energy Research was supported by the project "HVDC Inertia Provision (HVDC Pro)," funded by the ENERGIX Program of the Research Council of Norway, under Project 268053/E20, and the industry partners, Statnett, Equinor, RTE, and ELIA. (*Corresponding author: Jon Are Suul.*)

G. Bergna-Diaz was with EDF R&D while enrolled in both CentraleSupélec and NTNU. He is now with the Department of Electric Power Engineering, Norwegian University of Science and Technology (NTNU), 7491 Trondheim, Norway, (e-mails: gilbert.bergna@ntnu.no).

J. A. Suul is with SINTEF Energy Research, 7465 Trondheim, Norway, and also with the Department of Engineering Cybernetics, NTNU, 7491 Trondheim, Norway (e-mail: jon.a.suul@sintef.no).

E. Berne was with the Laboratoroy of Electrical Equipment, Electricité de France R&D (EDF R&D), 77818 Moret-sur-Loing, France. He is now with the Power System and Transmission Engineering Center (CIST) of the EDF Group, 93285 Saint-Denis, France (e-mail: erik.berne@edf.fr).

J.-C. Vannier is with GeePs (Group of electrical engineering-Paris), UMR CNRS 8507, CentraleSupelec, University of Paris-Sud, Université Paris-Saclay, Sorbonne Universités, UPMC Univ. Paris 06, 91192 Gif-sur-Yvette, France, (e-mail: jean-claude.vannier@centralesupelec.fr).

M. Molinas is with the Deptartment of EngineeringCybernetics, NTNU, 7491 Trondheim, Norway (email: marta.molinas@ntnu.no).

I. Introduction

For High Voltage *dc* (HVDC) transmission systems based on voltage source converter (VSC) technology, and especially for future multi-terminal systems, it will be important to avoid that power oscillations originating from the *ac* grid can propagate into the *dc* system [1], [2]. For power electronic converter topologies that do not contain internal energy storage elements between the *ac*- and *dc*-terminals, this can only be ensured by controlling the *ac*-side currents so that oscillations are eliminated from the instantaneous three-phase power flow at the *ac* terminals. Thus, control strategies for conventional two-level (2L) or three-level (3L) VSCs that are designed to eliminate double frequency active power oscillations from the power flow during operation with unbalanced grid voltage conditions will impose unbalanced *ac*-side currents [3]–[6]. The need for unbalanced ac-currents will also reduce the power transfer capability of the converter compared to operation with balanced three-phase currents, due to the limitations of the maximum phase current [5], [7]–[9].

Compared to 2L or 3L VSCs, the Modular Multilevel Converter (MMC) proposed in [10] introduces additional degrees of freedom in the control, due to its distributed internal capacitive energy storage. Especially, the possibility to control the internal circulating currents of an MMC separately from the the *ac*-side currents provides a flexibility in selecting the priority of the control objectives for the converter. For instance, the circulating currents can be controlled to be constant [11], or to contain a second harmonic component to compensate for second harmonic voltage or energy oscillations in each phase of the converter [12]. This flexibility can also be utilized during unbalanced grid voltage conditions, as discussed in numerous recent publications [13]. Thus, the MMC can be controlled to act as a *"power oscillation firewall"* or an *"energy buffer"* during unbalanced faults, preventing power oscillations on the *ac* side from propagating into the *dc* system. This can be achieved even if the *ac*-side currents are kept balanced during unbalanced conditions [14]–[20].

A. MMC energy buffering potential in unbalanced conditions

A simplified representation of a three phase MMC considered from a macroscopic perspective is sketched in Fig. 1. As indicated by this figure, each phase on the *dc*-side as well as the *ac*-side of an MMC can be represented by a controlled voltage source in series with an equivalent impedance. On the

This article has been accepted for publication in a future issue of this journal, but has not been fully edited. Content may change prior to final publication. Citation information: DOI 10.1109/JESTPE.2019.2894677, IEEE Journal of Emerging and Selected Topics in Power Electronics

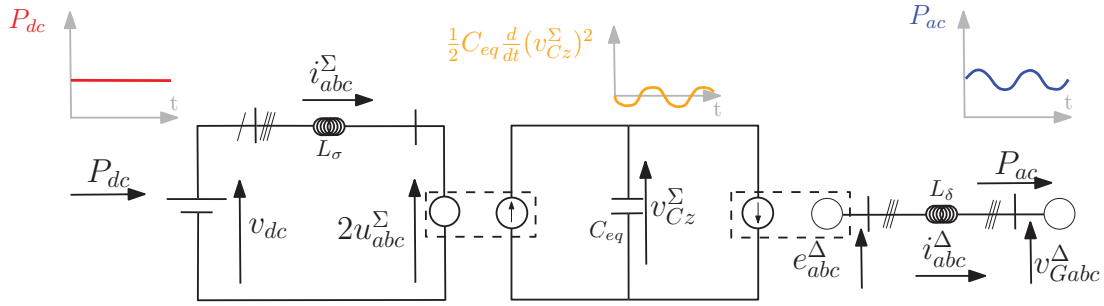

Fig. 1. Simplified representation of the MMC to emphasize its energy buffering capacity viewed from a macroscopic perspective.

dc-side, the currents in the equivalent interface impedance will be the circulating currents, i^{Σ}, of each phase, and the *dc*-side current, i_{dc}, will be equal to the sum of the circulating currents for all phases. As viewed from the *ac*- and *dc*-side terminals of an MMC model, the voltage sources would maintain a power balance with an internal, equivalent, capacitive energy storage [21].

A general model of a 2L-VSC with instantaneous power balance between the *ac*- and *dc*-terminals would be identical to the the right hand side of Fig. 1, i.e. the circuit representing the *ac* grid interconnection (e^{Δ}, i^{Δ}), and the "energy buffer circuit" (v^{Σ}_{Cz}). Indeed, for the 2L VSC, the capacitor voltage v^{Σ}_{Cz} in the figure would be the *dc*-side terminal voltage v_{dc}. Therefore, if power fluctuations due to unbalanced grid voltages should appear in the *ac*-side of the circuit at the point where the modulated voltage e^{Δ} is represented, they will unavoidably appear in v^{Σ}_{Cz} as well. Thus, such voltage and power fluctuations from a 2L VSC would propagate throughout the HVDC link. As already mentioned, this is usually avoided by controlling unbalanced *ac*-side currents so that no fluctuations will appear in the power flow at the *ac*-terminals.

Considering the full circuit sketched in Fig. 1, it can be immediately noticed that the equivalent internal voltage v^{Σ}_{Cz} of an MMC will not necessarily be identical to the *dc* voltage v_{dc}, as it will be for a 2L VSCs. Therefore, the MMC can be controlled so that the distributed capacitance of the MMC, as represented by the aggregate capacitor voltage v^{Σ}_{Cz} in Fig. 1, will function as an *energy buffer circuit* that can absorb power fluctuations or oscillations appearing at the *ac*-side. Thus, oscillation-free power flow at the *dc*-terminals under unbalanced *ac* grid voltage conditions does not inherently depend on unbalanced *ac*-side currents, as for the 2L VSC.

B. MMC capability for dc-side power control

From the simplified macroscopic MMC representation in Fig. 1, it can be argued that the equivalent internal energy buffer circuit and the possibility for independently controlling the *ac*-side and *dc*-side currents of an MMC can be utilized to completely decouple *any type* of undesired power fluctuations at the *ac*-side from propagating into the *dc*- side. In other words, there is no reason why such decoupling is only valid for steady-state power oscillations at twice the grid frequency that take place under unbalanced grid operation. If the MMC control objectives would be specified for this purpose, *any type* of power oscillations taking place at the *ac*-side, could be buffered by the internal energy storage and prevented from appearing at the *dc* terminals of the MMC, as long as the resulting oscillations in the internal capacitor voltages can be tolerated. Thus, the *ac*-side response to most transients phenomena, power perturbations as well as the steady state oscillations during unbalanced operation could potentially be blocked from propagating to the *dc*-side if the *dc*-side current or power of the MMC would be directly controlled by acting on the circulating currents of the MMC. Such an approach for control of the MMC will be different from the commonly applied control approach inherited from 2L or 3L VSCs, where the *ac*-side currents are utilized for controlling the power flow or the *dc*-voltage of an MMC-based HVDC converter station.

C. Context and contributions

Since the analysis and control of MMCs is currently being widely studied in the scientific community, several different methods have been proposed for controlling the circulating currents when operating under unbalanced grid voltage conditions [14]–[16], [18]–[20], [22]–[25]. However, many of the these proposed control strategies rely on a Circulating Current Suppression Controller (CCSC) and/or other control loops implemented in a synchronously rotating reference frame. Several proposals for control methods in the stationary reference frame are also utilizing the Clarke transformation for implementing control loops in αβ coordinates. Thus, such control methods are usually acting on the zero-sequence components of the three-phases for mitigating *dc*-side power oscillations of the MMC [14], [15], [22], [23]. Indeed, the utilization of the Clarke and/or Park transformations implies only indirect access to and control of per-phase quantities of MMC.

For providing direct and explicit control of phase quantities, an approach for circulating current control in *abc* phase-coordinates was proposed in [26], [27]. This control strategy was based on outer loop energy control and constrained mathematical optimization by the Lagrange multipliers method for derivation of the circulating current references, inspired by the work on active filters in [28], [29]. By designing the control directly in the *abc* frame, this approach provides the possibility for controlling the average values of MMC state variables in each phase to follow constant reference signals [26], [27], [30]. However, since the optimization problem formulated in [26] treated the phases of the MMC independently, the possibility for optimizing the operation of a three-phase converter under unbalanced *ac* grid voltage conditions was not considered.

This article has been accepted for publication in a future issue of this journal, but has not been fully edited. Content may change prior to final publication. Citation information: DOI 10.1109/JESTPE.2019.2894677, IEEE Journal of Emerging and Selected Topics in Power Electronics

A first attempt towards application of constrained mathematical optimization by the Lagrange multipliers method for shaping the circulating current references of a three-phase MMC to avoid *dc*-side power oscillations under unbalanced *ac* grid voltage conditions was presented in [30], [31]. In these initial efforts, the objective of avoiding *dc*-side power oscillations was conflicting with the constraints introduced in the optimization problem. Thus, dc-side power flow during unbalanced conditions was not precisely constant, although the oscillations could be significantly attenuated.

To achieve a flexible and versatile approach for controlling the MMC during unbalanced grid conditions, this paper presents a generalization of the approach in [26] that will ensure oscillation-free power flow at the *dc* terminals of the converter. This is achieved by including the requirement of oscillation-free *dc*-side power flow as a constraint in the formulation of the optimization problem defined for deriving the circulating current references. This results in a single analytic equation for calculating the references for the MMC circulating currents based on the output from a set of outer loop energy controllers. The resulting control approach is capable of regulating the energy stored inside the MMC whilst ensuring oscillation-free power at the *dc* terminals, considering two modes of operation with different control objectives defined as minimizing the oscillations of: i) the circulating current (i_k^{Σ}) or ii) the capacitive energy sum (w_{Ck}^{Σ}) of each phase k, for achieving reduced fluctuations in the MMC capacitor voltages.

The core idea behind the approach presented in this paper was first proposed in [12], and later utilized in [32]. The preliminary proposal in [12] is further refined here with a unified explanation of the derivations and an extended analysis of the impact of the proposed approach on the MMC operation, including evaluation of results from three different strategies for *ac*-side power control under unbalanced conditions, based on the following objectives [3], [4]: 1) constant active power with sinusoidal grid currents, 2) balanced grid currents and 3) constant reactive power with sinusoidal grid currents. The results in this paper and the corresponding analysis demonstrate how the various strategies for *ac*-side and circulating current reference calculation are influencing the energy and voltage oscillations of the MMC under unbalanced conditions. Furthermore, the effect of using the circulating currents to directly establish the desired steady state power flow of the converter according to the idea introduced in [12], is evaluated. This approach implies that the *ac*-side currents must be used to regulate the capacitive energy stored inside the MMC, instead of the more conventional approach of using the circulating currents to control the internally stored energy while the *ac*-side currents are used to establish the desired steady state power flow in the same way as for a 2L or 3L VSC. It will be shown that by using this strategy, the power flow at the *dc* terminals is most effectively decoupled from any transients originating from the *ac* grid, while the dynamic response to disturbances in the *ac* grid is only reflected in the control of the total energy stored in the MMC.

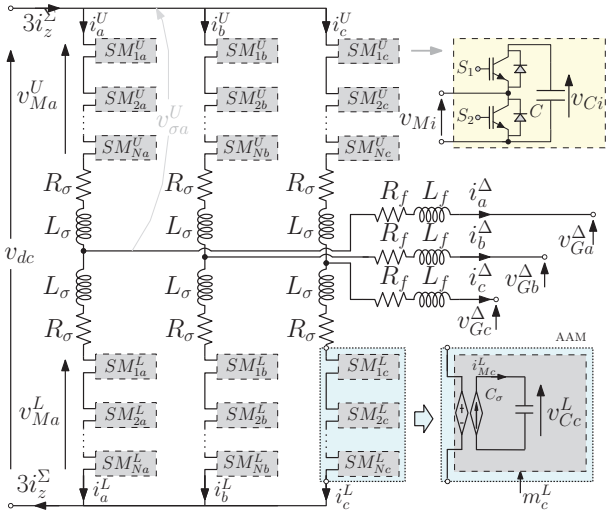

Fig. 2. Topology of the modular multilevel converter under consideration.

II. The Modular Multilevel Converter

The structure of a three-phase MMC is shown in Fig. 2. Each phase k of the converter is formed by $2N$ sub-modules (SMs) of which half of them are placed in the upper (U) arm and the other half in the lower (L). Each sub-module is composed by two switches (IGBT + diode) as shown in the same figure, and allows two active states: 1) bypassed, i.e. with zero voltage at the terminals or 2) inserted, i.e. with the capacitor voltage appearing at the terminals. Both upper and lower arms are constituted by an arm inductor—characterized by an inductance L_σ and a resistance R_σ— in order to compensate for voltage unbalances between the upper and lower multi-valves[1], and the *dc* terminal voltage. The *ac*-side interface is assumed to be a filter inductor and/or leakage inductance of a transformer, modeled by an equivalent resistance R_f and inductance L_f. For controller design and analysis, it is further assumed that that all the SMs in each arm can be replaced by a circuit-based arm average model (AAM), as indicated in Fig. 2 for the lower arm of phase *c* [33], [34]. Thus, each of the MMC arms appears as a controlled voltage source in the three-phase topology, while a power balance is established between the arm and its equivalent capacitance.

The *ac* grid side and circulating currents for a generalized phase k, i_k^{Δ} and i_k^{Σ}, are respectively defined in (1) and (2) as a function of the MMC upper and lower arm currents, i_k^U and i_k^L [11]:

$$i_k^{\Delta} = i_k^U - i_k^L \tag{1}$$

$$i_k^{\Sigma} = \frac{i_k^U + i_k^L}{2} \tag{2}$$

The dynamics of the aggregate capacitor voltages v_{Ck}^U and v_{Ck}^L used in the AAM representation of the MMC are given by:

$$\begin{aligned} C_\sigma \dot{v}_{Ck}^U &= m_k^U i_k^U, \\ C_\sigma \dot{v}_{Ck}^L &= m_k^L i_k^L, \end{aligned} \tag{3}$$

with m_k^U and m_k^L the upper and lower normalized arm insertion

[1] A multi-valve is here defined as the series interconnection of all the sub-modules in one arm.

This article has been accepted for publication in a future issue of this journal, but has not been fully edited. Content may change prior to final publication. Citation information: DOI 10.1109/JESTPE.2019.2894677, IEEE Journal of Emerging and Selected Topics in Power Electronics

indices of the converter, and $C_\sigma \triangleq C/N$. By further multiplying the above dynamical equations by their corresponding state variable (v^U_{Ck} or v^L_{Ck}), we get the upper and lower arm energy dynamics[2]

$$\begin{aligned} \dot{w}^U_{Ck} &= m^U_k v^U_{Ck} i^U_k, \qquad w^U_{Ck} \triangleq \frac{1}{2} C_\sigma \left(v^U_{Ck}\right)^2 = \frac{1}{2} C_\sigma \left(\sum_{i=1}^{N} v^U_{Cki}\right)^2, \\ \dot{w}^L_{Ck} &= m^L_k v^L_{Ck} i^L_k, \qquad w^L_{Ck} \triangleq \frac{1}{2} C_\sigma \left(v^L_{Ck}\right)^2 = \frac{1}{2} C_\sigma \left(\sum_{i=1}^{N} v^L_{Cki}\right)^2, \end{aligned} \tag{4}$$

The dynamics of the sum and difference of the capacitive energy ($w_{\Sigma k}$ and $w_{\Delta k}$) between the upper and lower arms (or multi-valves) are found by respectively adding and subtracting (4) [35], resulting in

$$\dot{w}^\Sigma_{Ck} = \dot{w}^U_{Ck} + \dot{w}^L_{Ck} = -e^\Delta_k i^\Delta_k + 2u^\Sigma_k i^\Sigma_k \tag{5}$$

$$\dot{w}^\Delta_{Ck} = \dot{w}^U_{Ck} - \dot{w}^L_{Ck} = \quad u^\Sigma_k i^\Delta_k - 2e^\Delta_k i^\Sigma_k \tag{6}$$

where e^Δ_k, and u^Σ_k are components of the internal modulated voltages of the MMC. These voltage components can be expressed as bilinear functions between the upper and lower insertion indexes m^U_k and m^L_k and the upper and lower capacitor voltages v^U_{Ck} and v^L_{Ck}, as given by

$$e^\Delta_k \triangleq \frac{m^L_k v^L_{Ck} - m^U_k v^U_{Ck}}{2} \tag{7}$$

$$u^\Sigma_k = \frac{m^U_k v^U_{Ck} + m^L_k v^L_{Ck}}{2} \tag{8}$$

III. Optimal shaping of the MMC circulating currents

An approach for calculating the MMC circulating current references directly in the *abc* phase coordinates, based on constrained mathematical optimization by means of the Lagrange multipliers method, was presented in [26]. In order to make the following discussions self-contained, the derivation originally presented in [26] is first briefly recalled before introducing the required analysis for ensuring oscillation-free dc-side power flow of a three-phase MMC.

A. Phase-independent optimization of the circulating current references

For simplicity, it is assumed in the following derivations that $u^\Sigma_k \approx \frac{v_{dc}}{2}$. Furthermore, u^Σ_k as well as e^Δ_k and i^Δ_k will be considered as measurable disturbances in equations (5)-(6). These considerations are based on the assumption of time-scale separation between the circulating current control and 1) all outer control loops and energy dynamics and 2) the closed loop *ac*-side current dynamics.

[2]Notice that the energy definitions introduced here differ in general from the *real physical* arm energy dynamics, which are found by adding up all the SM energies, except for the case in which a fast balancing algorithm is assumed which forces equal SM voltages within the arm. Nonetheless, from a control design perspective, these *virtual* energy definitions can always be considered as the result of an appropriate change of coordinates which accurately maps the original capacitor voltage dynamics (3).

Let $f_k\left(i^\Sigma_k\right)$ be the objective function[3] (associated to the converter phase k), expressed as:

$$f_k\left(i^\Sigma_k\right) = \alpha \frac{1}{T} \int_{to}^{to+T} (\dot{w}^\Sigma_{Ck})^2 dt + (1-\alpha) \frac{1}{T} \int_{to}^{to+T} \left(v_{dc} i^\Sigma_k\right)^2 dt \tag{9}$$

This objective function consists of the two following conflicting objectives [26] :

(i) Minimize the power oscillations associated to the capacitive energy sum variable w^Σ_{Ck}. This objective is represented by the first integral on the right hand side of the equality in (9).

(ii) Minimize the oscillations of the power flow associated with the circulating current i^Σ_k. This objective is represented by the second integral on the right hand side of the equality in (9).

Thus, a weighting factor $\alpha \in [0,1]$ is used to balance their conflicting nature.

The objective function in (9) is subject to two constraints, associated with horizontal and vertical energy balancing control of the MMC. More precisely, for each phase k, the constraint given in (10) is defined to regulate the average of the energy sum, whereas the constraint given in (11) is defined to regulate the average value of the energy difference.

$$\frac{1}{T} \int_{to}^{to+T} \left(\dot{w}^\Sigma_{Ck}\right) dt \equiv \overline{P^*_{\Sigma k}} \tag{10}$$

$$\frac{1}{T} \int_{to}^{to+T} \left(\dot{w}^\Delta_{Ck}\right) dt \equiv \overline{P^*_{\Delta_k}} \tag{11}$$

In (10) and (11), $\overline{P^*_{\Sigma k}}$ and $\overline{P^*_{\Delta k}}$ are assumed to be determined by PI controllers for regulating the average values of the energy sum and difference ($\overline{w}^\Sigma_{Ck}$ and $\overline{w}^\Delta_{Ck}$) to their desired references, as given by:

$$\overline{P^*_{\Sigma k}} \triangleq \left[k^\Sigma_P \left(\overline{w}^{\Sigma\text{ref}}_{Ck} - \overline{w}^\Sigma_{Ck}\right) + k^\Sigma_I \int \left(\overline{w}^{\Sigma\text{ref}}_{Ck} - \overline{w}^\Sigma_{Ck}\right) dt\right] \tag{12}$$

$$\overline{P^*_{\Delta k}} \triangleq \left[k^\Delta_P \left(\overline{w}^{\Delta\text{ref}}_{Ck} - \overline{w}^\Delta_{Ck}\right) + k^\Delta_I \int \left(\overline{w}^{\Delta\text{ref}}_{Ck} - \overline{w}^\Delta_{Ck}\right) dt\right] \tag{13}$$

From (9), (10) and (11), the *Lagrangian* $\mathcal{L}$ associated with the optimization problem under consideration is defined as:

$$\begin{aligned} \mathcal{L}(i^\Sigma_k, \lambda_\Sigma, \lambda_\Delta) \triangleq \; & \alpha \frac{1}{T} \int_{to}^{to+T} (\dot{w}^\Sigma_{Ck})^2 dt \\ & + (1-\alpha) \frac{1}{T} \int_{to}^{to+T} \left(v_{dc} i^\Sigma_k\right)^2 dt \\ & + \lambda_\Sigma \left(\frac{1}{T} \int_{to}^{to+T} \dot{w}^\Sigma_{Ck} dt - \overline{P^*_{\Sigma_k}}\right) \\ & + \lambda_\Delta \left(\frac{1}{T} \int_{to}^{to+T} \dot{w}^\Delta_{Ck} dt - \overline{P^*_{\Delta_k}}\right) \end{aligned} \tag{14}$$

with λ_Σ and λ_Δ the so-called *Lagrange multipliers*. A solution to this optimization problem is possible since the two selected constraints are compatible: i.e., according to [33], [35] the average value of the energy sum ($\overline{w}^\Sigma_{Ck}$) depends on the *dc* component of the circulating current, while the average value

[3]Notice that the dependence of the objective function only on i^Σ_k is a direct consequence of the underlying assumption given above.

This article has been accepted for publication in a future issue of this journal, but has not been fully edited. Content may change prior to final publication. Citation information: DOI 10.1109/JESTPE.2019.2894677, IEEE Journal of Emerging and Selected Topics in Power Electronics

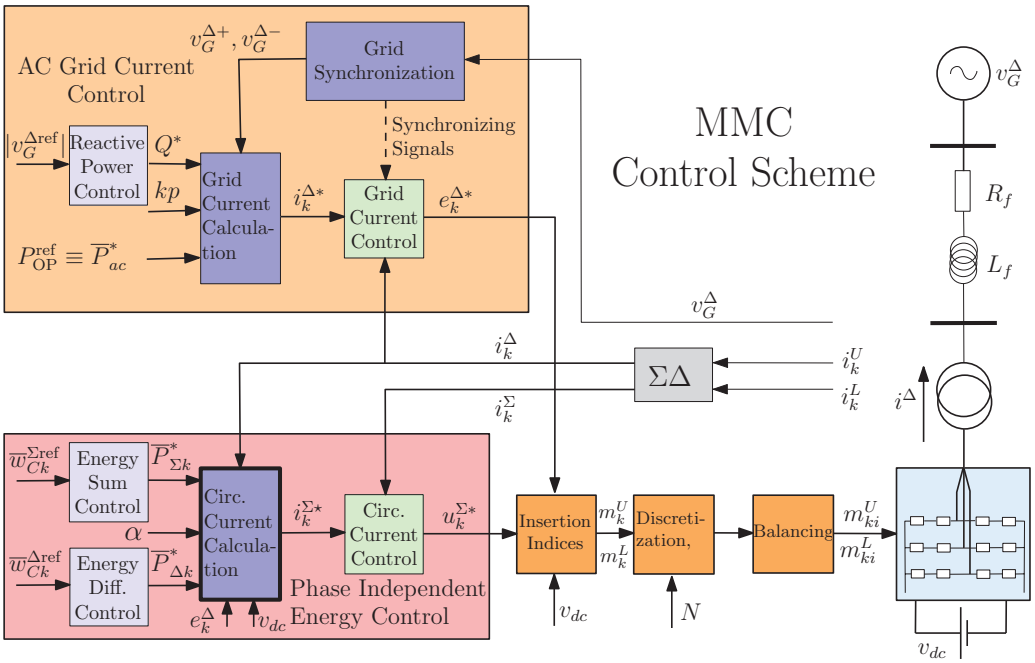

Fig. 3. MMC Phase Control Scheme [26]

of the energy difference ($\overline{w}_{Ck}^{\Delta}$) depends on the fundamental frequency component of the circulating current. These constraints will participate in the shaping of the circulating current reference, by defining its *dc*-component and its grid frequency component, respectively according to the above analysis. Nonetheless, there are still sufficient degrees of freedom regarding the component at twice the grid frequency. This component is directly associated to the objective functions, and will depend on the weighting factor selected.

Differentiating the Lagrangian with respect to the circulating current variable and both of the Lagrange multipliers λ_Σ and λ_Δ,

$$\nabla_{\left(i_k^{\Sigma},\lambda_\Sigma,\lambda_\Delta\right)} \mathcal{L}\left(i_k^{\Sigma},\lambda_\Sigma,\lambda_\Delta\right) = 0 \tag{15}$$

and solving the resulting three dimensional equation system (see [26] for more details), the circulating current reference can be obtained as:

$$i_k^{\Sigma\star} = \overbrace{\frac{\overline{P}_{\Sigma k}^{*} + (1-\alpha)\,\overline{e_k^{\Delta} i_k^{\Delta}}}{v_{dc}^2} \cdot v_{dc}}^{\sim dc} + \overbrace{\frac{\alpha}{v_{dc}} \cdot e_k^{\Delta} i_k^{\Delta}}^{\sim 2\omega} + \overbrace{\frac{-\overline{P}_{\Delta k}^{*}}{2v_{dc}^2\left(e_{k,\text{p.u.}}^{\Delta,\text{rms}}\right)^2} \cdot e_k^{\Delta}}^{\sim \omega} \tag{16}$$

where $\overline{e_k^{\Delta} i_k^{\Delta}}$ and $e_k^{\Delta} i_k^{\Delta}$ are the average and instantaneous values of the *ac*-side power calculated from the product between the *ac*-side current i_k^{Δ} and the internal voltage e_k^{Δ} of phase k. In addition,

$$\left(e_{k,\text{p.u.}}^{\Delta,\text{rms}}\right)^2 \triangleq \frac{1}{T}\int_{to}^{to+T}\left(\frac{e_k^{\Delta}}{v_{dc}}\right)^2 dt.$$

The first term on the right hand side of the equal sign in (16) is the *dc* component of the circulating current, which is responsible for regulating the average value of the capacitive energy sum of each phase ($\overline{w}_{Ck}^{\Sigma}$) and ensures the average power balance[4]. The second term in (16) is the second harmonic component of the circulating current that ensures constant energy sum ($w_k^{\Sigma} \equiv 0$) in steady state when $\alpha = 1$, whereas the last term is a fundamental frequency component that will regulate the average energy difference between the upper and lower arms ($\overline{w}_{Ck}^{\Delta}$). The assumed control structure of an MMC, including the implementation of the circulating current reference (16) is sketched in Fig. 3—see [26] for more details. It is also worth mentioning that the formulation in (16) allows to control the energy stored in the equivalent arm capacitors of the converter—through $\overline{P}_{\Sigma k}^{*}$ and $\overline{P}_{\Delta k}^{*}$—independently of the value of the voltage v_{dc} at the dc terminals of the MMC.

B. Optimal circulating current reference shaping for unbalanced operation

The circulating current reference $i_k^{\Sigma\star}$ expressed in (16) is the solution to the optimization problem formulated in the previous subsection. Nonetheless, it can be easily noticed that the sum of the three phases ($\sum_{k\in abc} i_k^{\Sigma\star}$) is not being explicitly controlled to become a constant variable in steady-state operation, due to the fact that the optimization problem was formulated independently per phase. Hence, the *dc* power output will not necessarily become constant or oscillation-free. For preventing oscillations originating from the *ac*-side operation of the MMC to propagate into the *dc*-side the optimization problem must be reformulated by considering all three phases. Thus, the following new constraint is defined [12]:

$$v_{dc}\sum_{k\in(abc)} i_k^{\Sigma} \equiv \overline{P}_{dc}^{*}. \tag{17}$$

[4]Recall that the average value of the circulating current is related to the average power transfer between the *ac* and *dc* sides.

This article has been accepted for publication in a future issue of this journal, but has not been fully edited. Content may change prior to final publication. Citation information: DOI 10.1109/JESTPE.2019.2894677, IEEE Journal of Emerging and Selected Topics in Power Electronics

In the above equation, $\overline{P}^*_{dc}$ will be a constant or oscillation-free power reference. How this power reference can be chosen is discussed in section V.

1) Conflicting constraints: The constraint in (17) is not compatible with the constraints (10) and (11) used to determine $i_k^{\Sigma\star}$. The reason is that these constraints were responsible for the the *dc*-component and the fundamental frequency components of i_k^{Σ} that are needed in order to achieve the desired energy regulation, while the new constraint in (17) is imposing a relation between the phases, *including* the *dc*-components of i_k^{Σ}. To overcome this issue, one of the constraints directly associated to the *dc* value of i_k^{Σ} must be relaxed.

For ensuring that power oscillations at the *dc*-terminals will be suppressed, the constraint in (17) must be prioritized. Even though the energy regulation provided by equations (10) and (11) is quite important to maintain the desired operating conditions of the system, these constraints can be relaxed in order to find a new circulating current reference $i_k^{\Sigma\ddagger}$. This is achieved by shifting the equations that were initially constraints, to become part of a new objective function.

2) Mathematical derivation: The optimization problem is defined in the following way. The desired shape of the circulating current of each phase will be *as similar as possible* to $i_k^{\Sigma\star}$; subject to the constant power constraint given in (17). More precisely, the *new* objective function $f(i_k^{\Sigma})$ is now given as

$$f(i_k^{\Sigma}) = [i_k^{\Sigma} - i_k^{\Sigma\star}]^2 \tag{18}$$

where $i_k^{\Sigma\star}$ is the optimal circulating current reference previously calculated in (16). Notice that due to the derivation procedure of $i_k^{\Sigma\star}$ and its appearance in (18), the new objective function also contains the information of the constraints (10) and (11) used in the previous formulation. However, they are not imposed as *strict* constraints, since they appear in the objective function $f(i_k^{\Sigma})$. Thus, these constraints have now been *relaxed*. On the other hand, the only *strict* constraint considered in this new formulation is the one associated to constant power flow at the MMC *dc* terminals defined in (17).

The *Lagrangian* associated to this new optimization problem is now defined as

$$\mathcal{L}\left(i_k^{\Sigma},\lambda\right) = \left(i_k^{\Sigma} - i_k^{\Sigma\star}\right)^2 + \lambda\left(v_{dc}\sum_{k\in(abc)} i_k^{\Sigma} - \overline{P}^*_{dc}\right). \tag{19}$$

Here again, it can be concluded from a simple analysis that the solution for this optimization problem is feasible. Even though one constraint appears, it does not define entirely the shape of the circulating current. More precisely, it only ensures that the sum of the circulating currents for all phases phases (times v_{dc}) will be free from oscillations. Therefore, there is still a sufficient degrees of freedom regarding the individual waveforms of the circulating currents in each phase, which is used to minimize the new objective function.

To obtain the new circulating current reference $i_k^{\Sigma\ddagger}$, it is necessary to analytically solve $\nabla_{\left(i_k^{\Sigma},\lambda\right)}\mathcal{L}\left(i_k^{\Sigma},\lambda\right) = 0$. Differentiating $\mathcal{L}\left(i_k^{\Sigma},\lambda\right)$ with respect to i_k^{Σ}, results in

$$\frac{\partial\mathcal{L}}{\partial i_k^{\Sigma}} = 2\left(i_k^{\Sigma} - i_k^{\Sigma\star}\right) + \lambda v_{dc} = 0. \tag{20}$$

Similarly, differentiating $\mathcal{L}\left(i_k^{\Sigma},\lambda\right)$ with respect to λ, results in

$$\frac{\partial\mathcal{L}}{\partial\lambda} = v_{dc}\sum_{k\in(abc)} i_k^{\Sigma} - \overline{P}^*_{dc} = 0. \tag{21}$$

Multiplying (20) by $\frac{v_{dc}}{2}$, adding all three phases and combining the resulting equation with (21) yields in

$$\lambda = \frac{v_{dc}\sum_{k\in(abc)} i_k^{\Sigma\star} - \overline{P}^*_{dc}}{\frac{3}{2}v_{dc}^2}. \tag{22}$$

Replacing (22) in (20) results in the new circulating current reference equation $i_k^{\Sigma\ddagger}$, given as

$$i_k^{\Sigma\ddagger} = i_k^{\Sigma\star} - \frac{1}{3}\sum_{k\in(abc)} i_k^{\Sigma\star} + \frac{1}{3}\frac{\overline{P}^*_{dc}}{v_{dc}}. \tag{23}$$

Notice that (23) has the following clear physical interpretation. The *original* zero-sequence component of the circulating current, $i_z^{\Sigma\star} \triangleq \frac{1}{3}\sum_{abc} i_k^{\Sigma\star}$, is being subtracted from the reference and replaced by the new component $i_z^{\Sigma\ddagger} \triangleq \frac{1}{3}\overline{P}^*_{dc}/v_{dc}$. Indeed, the *new* zero sequence component of the circulating current $i_z^{\Sigma\ddagger}$ has as its only objective to ensure constant power flow at the *dc* terminals of the MMC, without contributing to the phase-independent arm capacitor energy regulation. Consequently, the phase-independent arm capacitor energy regulation will be carried out only by the non-zero-sequence components of the circulating currents; i.e., by $i_k^{\Sigma\ddagger} - i_z^{\Sigma\ddagger}$.

Replacing $i_k^{\Sigma\star}$ from (16) into (23) provides the full expression for the circulating current reference as:

$$\begin{aligned} i_k^{\Sigma\ddagger} =& \frac{\overline{P}^*_{\Sigma k} + (1-\alpha)\cdot\overline{e_k^{\Delta} i_k^{\Delta}}}{v_{dc}^2}v_{dc} + \frac{\alpha\cdot e_k^{\Delta} i_k^{\Delta}}{v_{dc}} + \frac{-\overline{P}^*_{\Delta k} e_k^{\Delta}}{2v_{dc}^2\left(e_{k,\text{p.u.}}^{\Delta,\text{rms}}\right)^2} \\ &- \sum_{k\in(abc)}\left(\frac{\overline{P}^*_{\Sigma k} + (1-\alpha)\cdot\overline{e_k^{\Delta} i_k^{\Delta}}}{v_{dc}^2}v_{dc} + \frac{\alpha\cdot e_k^{\Delta} i_k^{\Delta}}{v_{dc}}\right. \\ &\left. + \frac{-\overline{P}^*_{\Delta k} e_k^{\Delta}}{2v_{dc}^2\left(e_{k,\text{p.u.}}^{\Delta,\text{rms}}\right)^2}\right) + \frac{1}{3}\frac{\overline{P}^*_{dc}}{v_{dc}}. \end{aligned} \tag{24}$$

It can be seen from this equation that the sum of the circulating current references for the three phases will always yield in $\frac{\overline{P}^*_{dc}}{v_{dc}}$, regardless of the phase independent energy regulation action that i_k^{Σ} is performing. Moreover, by adequately choosing $\overline{P}^*_{dc}$, the output *dc* power of the converter may be controlled to effectively prevent oscillations from the *ac*-side from propagating into the *dc*-side.

It is worth mentioning that the implementation of (24) is rather straightforward regardless of the complexity of the derivation. This is because (24) mainly relies on algebraic expressions and standard averaging techniques, in addition to the output signals from the PI controllers for the energy balancing control, as defined by (12) and (13). Furthermore, notice that (24) simplifies even further when selecting one of the frontier cases $\alpha \equiv 1$ or $\alpha \equiv 0$.

IV. Assumed control system implementation

The expression for the optimized circulating current reference given by (24) can be utilized in any MMC control

This article has been accepted for publication in a future issue of this journal, but has not been fully edited. Content may change prior to final publication. Citation information: DOI 10.1109/JESTPE.2019.2894677, IEEE Journal of Emerging and Selected Topics in Power Electronics

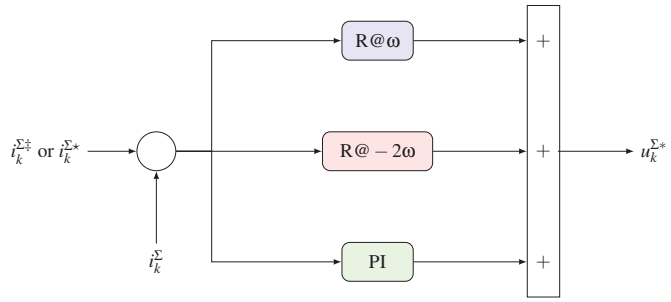

Fig. 4. Multi-Resonant Shunt Control Structure for the Circulating Current

system configuration relying on separate control of ac-side and circulating currents. The control system implementation assumed for the analysis in this paper is presented in following.

A. Circulating current control by stationary multi-resonant controllers

The circulating current references resulting from the mathematical optimization in the previous section provides the theoretical optimal currents for regulating the arm capacitive energies independently for each phase, while ensuring non-oscillatory power at the *dc*-terminals of the converter. For utilizing the optimal current reference from (24) in a control system, it should be noticed that this equation for each phase k will contain three different harmonic components—a *dc* component proportional to v_{dc}, a fundamental frequency component, and a second harmonic component. Thus, a suitable and simple approach for implementing the circulating current control is to use multiple stationary frame *resonant* controllers [36], [37] tuned for controlling the individual frequency components. Such resonant controllers have been widely studied as an interesting alternative to the use of synchronous reference frame PI controllers, in order to avoid the computational load of implementing multiple synchronous reference frame transformations [37]. Recently, resonant controllers have also been widely applied to MMC circulating current control, as for instance discussed in [17]–[19].

The multi-resonant controller structure implemented in this work is depicted in Fig. 4. It consists on the direct addition of two single resonant controllers at once and twice the grid frequency with a common proportional-integral (PI) term (referred to as parallel or shunt configuration [37]). This structure corresponds to the *circulating current control* block of the control scheme from Fig. 3. For considering operation of the system under grid frequency variations, frequency-adaptive Second Order Generalized Integrators (SOGIs) can be utilized to implement the resonant terms of the current controller [38].

B. AC-side current reference calculation and control

For evaluating MMC operation under unbalanced grid voltage conditions, it is also necessary to define a strategy for shaping the active and reactive power flow on the ac-side of the MMC. As mentioned in the introduction, the performance of the MMC with the presented approach for circulating current reference calculation is evaluated in this paper for different power control strategies applied to the control of the *ac*-side currents. For simplicity, the investigation is limited to the case of active power control, and the corresponding three-phase current references are calculated according to the following generalized equation [4]:

$$i_k^{\Delta*} = \frac{\overline{P}_{ac}^{*}}{\left\|\mathbf{v}_G^{\Delta+}\right\|^2 + kp\cdot\left\|\mathbf{v}_G^{\Delta-}\right\|^2}\cdot\left(v_{Gk}^{\Delta+} + kp\cdot v_{Gk}^{\Delta-}\right) \tag{25}$$

In (25), $\overline{P}_{ac}^{*}$ is the power reference at the *ac* point of common coupling (PCC), and v_{Gk}^{+} and v_{Gk}^{-} are the positive and negative sequence components of the phase k voltage measured at the point of common coupling. For further detailes, please refer to [3], [4]. Three different cases are investigated, corresponding to the following objectives for controlling the power flow characteristics at the point of synchronization to the *ac* grid:

- Elimination of double frequency oscillations in the *ac* power flow while maintaining sinusoidal currents: current reference calculation by equation (25) with $kp = -1$
- Balanced sinusoidal *ac* currents: current reference calculation by equation (25) with $kp = 0$
- Elimination of double frequency reactive power oscillations at the point of synchronization to the grid: current reference calculation by equation (25) with $kp = +1$

The *ac*-side phase currents are controlled to follow the current references resulting from (25) by using resonant controllers implemented in the stationary $\alpha\beta$ reference frame according to [36], [39]. The output from the current controllers will, after transformation from $\alpha\beta$ to *abc* coordinates, provide the voltage references $e_k^{\Delta*}$ as indicated in Fig. 5. The synchronization to the *ac* voltage at the PCC and the detection of positive and negative sequence components of the grid voltage is based on Dual SOGIs configured as quadrature signal generators (DSOGI-QSG) according to [40].

It should be noted that the grid synchronization and the control of the ac-side power flow is based on methods and techniques that are well established and widely studied for grid connected 2L VSCs. Thus, the applied control strategy can be easily adapted to handle additional practical challenges related to grid connected operation. For instance, the grid synchronization mechanism based on the DSOGI-QSG is inherently frequency-adaptive, and can be extended to include harmonic sequence decomposition, as proposed in [7]. Similarly, strategies for limiting the power flow and current references resulting from (25) can be introduced to ensure safe operation of the converter during severe ac-side grid faults, as discussed in [5], [9], [39].

V. Power Flow Control and Definition of Roles for AC- and DC-Side Power References

From the equation for the circulating current reference $i_k^{\Sigma\ddagger}$ given in (24), and the equation for the *ac*-side current reference $i_k^{\Delta*}$ given in (25), it is clear that it is possible to define the *dc* power reference $\overline{P}_{dc}^{*}$ and the *ac* power reference $\overline{P}_{ac}^{*}$ separately as explicit signals within the control system. However, to preserve the system stability only one of these references can be used to define the steady-state power flow of the converter, while the other reference must be utilized to compensate for

This article has been accepted for publication in a future issue of this journal, but has not been fully edited. Content may change prior to final publication. Citation information: DOI 10.1109/JESTPE.2019.2894677, IEEE Journal of Emerging and Selected Topics in Power Electronics

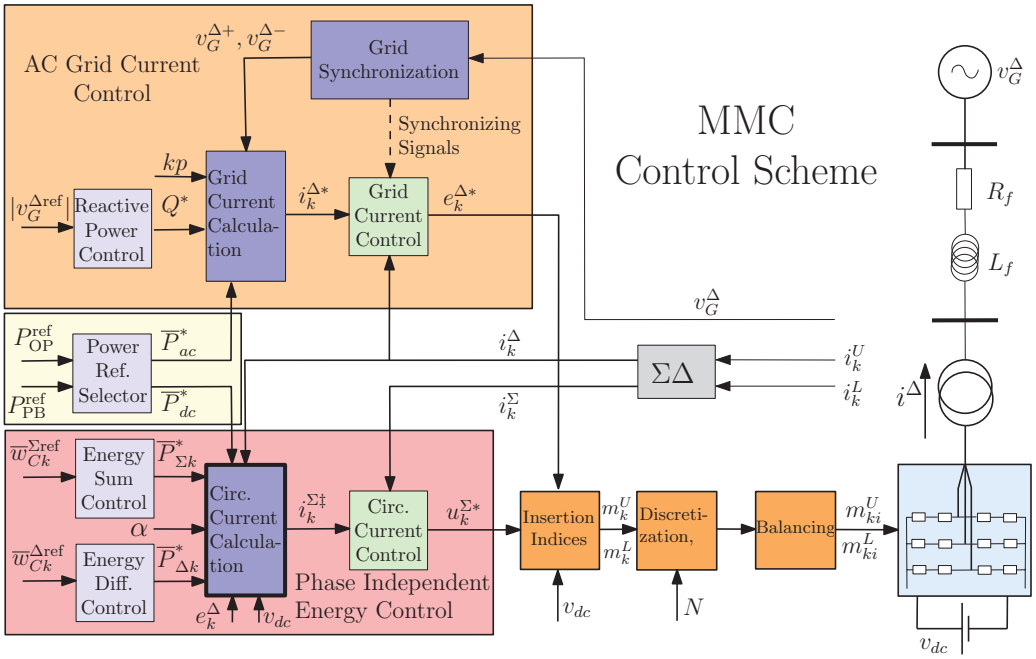

Fig. 5. Schematic diagram of the proposed control

the internal losses while balancing the total energy stored within the converter.

To simplify the analysis, consider as an example an MMC operating as a *constant power controlled HVDC converter station*. This implies that it will be necessary to assign the constant power reference corresponding to the desired operating point (OP), $P^{\text{ref}}_{\text{OP}}$, to *one of the two* available active powers; i.e., $\overline{P}^{*}_{ac}$ or $\overline{P}^{*}_{dc}$. Furthermore, the remaining one of the two active powers that is *not* being used to force the desired constant power operating point, is then assigned to the objective of *ensuring the power balance* (PB) of the converter by *regulating its average capacitve energy sum*. This power reference, $P^{\text{ref}}_{\text{PB}}$, can be generated by a PI controller as

$$P^{\text{ref}}_{\text{PB}} = k_P\left(\overline{w}^{\Sigma\text{ref}}_{C3\phi} - \overline{w}^{\Sigma}_{C3\phi}\right) + k_I\int\left(\overline{w}^{\Sigma\text{ref}}_{C3\phi} - \overline{w}^{\Sigma}_{C3\phi}\right)dt \qquad (26)$$

where $\overline{w}^{\Sigma\text{ref}}_{C3\phi}$ is the desired reference for the three-phase average capacitive energy $\overline{w}^{\Sigma}_{C3\phi}$. Thus, as first suggested in [12] this degree of freedom allows for the following two different ways of controlling the MMC.

1) **Case A:** $\overline{P}^{*}_{ac} = P^{\text{ref}}_{\text{OP}}$ and $\overline{P}^{*}_{dc} = P^{\text{ref}}_{\text{PB}}$
   This applies the same approach for power flow control as in a 2L VSC converter (where there is only one degree of freedom; i.e., the desired power transfer). Thus the constant power operating point will be established by $\overline{P}^{*}_{ac}$, whereas the *dc*-side power reference $\overline{P}^{*}_{dc}$ is used to regulate the average value of the capacitive energy of the MMC, by means of (26).
2) **Case B:** $\overline{P}^{*}_{dc} = P^{\text{ref}}_{\text{OP}}$ and $\overline{P}^{*}_{ac} = P^{\text{ref}}_{\text{PB}}$
   In this case, the desired constant power operating point is established by means of the *dc*-side power reference $\overline{P}^{*}_{dc}$, while the *ac*-side power reference $\overline{P}^{\text{ref}}_{ac}$ will be defined by (26). This case is of significant interest, since the MMC will not only decouple the *ac*-side power fluctuations from the *dc*-side power fluctuations in steady state (as in the previous case), but also buffer the impact of any *ac*-side transients as well. This behaviour will be similar to a *stiff dc current/power source*, and will be illustrated and further analyzed in section VI-C.

The resulting control scheme is depicted in Fig. 5. As can be seen, the control of the constant power operating point $P^{\text{ref}}_{\text{OP}}$ of the system is no longer necessarily actuated by the *ac*-side currents, illustrated by the presence of the additional *power reference selector* block. Indeed, this new block emphasizes the possibility of switching between the configurations defined above as **Case A** and **Case B**.

The two different approaches for power control presented above can be easily extended to the case of *dc* voltage controlled or *dc* droop-controlled HVDC converter stations. Indeed, if an additional outer loop *dc* voltage controller is designed to provide $P^{\text{ref}}_{\text{OP}}$, the presented strategy for optimal shaping of the circulating current references as well as the two options for organizing the power flow control and energy balancing will be equally applicable as for the assumed example. However, it can be mentioned that the choice of which controller provides $\overline{P}^{*}_{ac}$ and $\overline{P}^{*}_{dc}$ can have significant influence on the dynamic response and controller bandwidth, especially for the case of dc voltage control. A preliminary evaluation of this issue, based on a different control strategy and a simplified MMC model, was presented in [41]. The results from this study showed how a control system configuration with a dc-voltage controller providing $\overline{P}^{*}_{ac}$ implies that the closed loop response of the controller for the capacitive energy sum given by (26) will limit the bandwidth of the dc-voltage controller. Thus, the same limitations will apply to the overall control strategies assumed in this paper. This also implies that the configuration of the energy balancing and power flow control of an MMC can have significant impact on the potential for

This article has been accepted for publication in a future issue of this journal, but has not been fully edited. Content may change prior to final publication. Citation information: DOI 10.1109/JESTPE.2019.2894677, IEEE Journal of Emerging and Selected Topics in Power Electronics

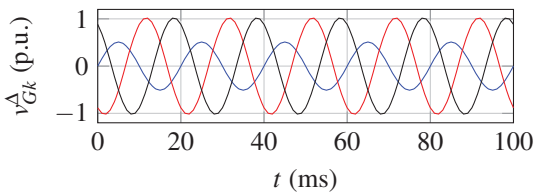

Fig. 6. Unbalanced grid voltage

utilizing internally stored energy and/or power from the dc-side to provide inertial response from an MMC HVDC terminal. Thus, previous studies of inertia emulation and control of HVDC terminals as virtual synchronous machines (VSMs), based on 2L VSCs [42] or on MMCs with conventional CCSC [43], will not provide accurate representation of MMCs with closed loop control of the dc-side current and/or the internally stored energy.

VI. Simulation of MMC operation under unbalanced conditions

In this section, time-domain simulation results for a three phase MMC with the parameters from Table 1, operating under unbalanced conditions are presented and evaluated. The MMC parameters are inspired from the preliminary design of the MMC-HVDC system between France and Spain presented in [44], with 400-SMs per arm, and SM capacitance designed for a stored energy equivalent to 30 kJ/MVA. In addition, the case of a single phase fault in phase *a* of the equivalent grid voltage source as shown in Fig. 6 is investigated. For the simulations, an MMC working in constant power control mode is assumed to be connected to a stiff *dc* voltage source [5]. The control system of the MMC is implemented according to Fig. 5, and all the required input signals for the calculation of the circulating current references have been estimated using adaptive filters based on SOGI-QSGs, as explained in [45].

For simplicity, the time-domain simulation results presented in the following section are based on the averaged arm model (AAM) of the converter. For simulation with an AAM representation of the MMC, each arm is represented by a controlled voltage source which is coupled with an equivalent arm capacitance that represents the internal arm voltage dynamics. Further validation and analysis of such models are available in [33], [34], [46], [47], but it should be noted that the model includes nonlinear effects except for the switching operations and the dynamics of the SM capacitor voltage balancing algorithm. The model is simulated in Matlab/Simulink with the SimPowerSystem toolbox.

A. Simulation results with the phase-independent formulation of [26]

The approach for circulating current reference calculation proposed in this paper in (23), (24) stems from the need of a general equation capable of ensuring constant *dc* power during unbalanced operation. This subsection intends to briefly illustrate via time-domain simulations the limits of the phase-independent formulation of [26] recalled in (16), under unbalanced grid voltage conditions. The main variables of interest from simulation results with this control strategy are depicted in Fig. 7, when the MMC is exposed to the unbalanced grid voltages from Fig. 6. While the circulating current references are calculated by (16) the grid current references are calculated with (25), with $kp = 0$ for ensuring balanced *ac*-side currents during the unbalanced operation.

For the simulated scenario, Fig. 7 shows the three phase *ac*-side currents, the instantaneous three-phase active power, the capacitive energy sum stored in each phase of the converter, and the instantaneous power at the *dc* terminals of the MMC, the sum of the capacitor voltages for each arm, the circulating currents, the energy difference between arms per phase and the instantaneous reactive power. In addition, the figure is showing the results of using equation (16) with the two frontier values of α in order to evaluate the performance under both modes of operation: minimizing the oscillations of the circulating current ($\alpha = 0$) and minimizing the oscillations of the capacitive energy sum per phase ($\alpha = 1$).

Since there is an unbalance in the *ac* grid voltage, and the *ac*-side currents are controlled to be balanced, the instantaneous active power at the *ac*-side has a pronounced 2ω oscillation. When $\alpha = 1$, the power fluctuations that are observed at the *ac*-side can be also found in the *dc*-side power as well. For this case it is clear that equation (16) is not enough to guarantee oscillation-free power at the *dc* terminals. Nonetheless, for the case of $\alpha = 0$, the circulating current is being minimized and therefore contributes to minimizing the oscillations of the *dc* power as well[6]. However, it is worth emphasizing that even though the *dc* power fluctuations are small, they are only implicitly attenuated by the phase-independent control.

TABLE I: MMC Parameters [44]

Parameter	Value
Number of SM per arm	400
Nominal *dc* terminal voltage	640 kV
Nominal *ac* terminal voltage	266.4 kV
Nominal power	1059 MVA
Sub-Module capacitance	10 mF
Equivalent arm capacitance	0.025 mF
Arm inductance	50 mH
Arm resistance	10 $m\Omega$

B. Simulation results with presented formulation suitable for unbalanced operation

In this section, operation with circulating current reference calculation by (24) is being evaluated under the three different *ac*-side current control strategies, corresponding to oscillation-free *ac* active power ($kp = -1$), balanced *ac*-side currents

[5]As mentioned earlier, the investigation could be easily extended to MMCs in *dc* voltage controlling mode or droop-controlled mode, interfacing a constant *dc* current source or a multi-terminal HVDC system instead. However, since the emphasis of this work is the unbalanced *ac*-grid conditions, the case of an MMC interfacing a stiff dc voltage source operating in constant power mode is preferred for simplicity.

[6]Recall that the sum of the circulating currents ($\sum_{k\in(abc)} i_{ck}$) will produce the dc-side current, which in turn is associated with the *dc*-side power flow.

This article has been accepted for publication in a future issue of this journal, but has not been fully edited. Content may change prior to final publication. Citation information: DOI 10.1109/JESTPE.2019.2894677, IEEE Journal of Emerging and Selected Topics in Power Electronics

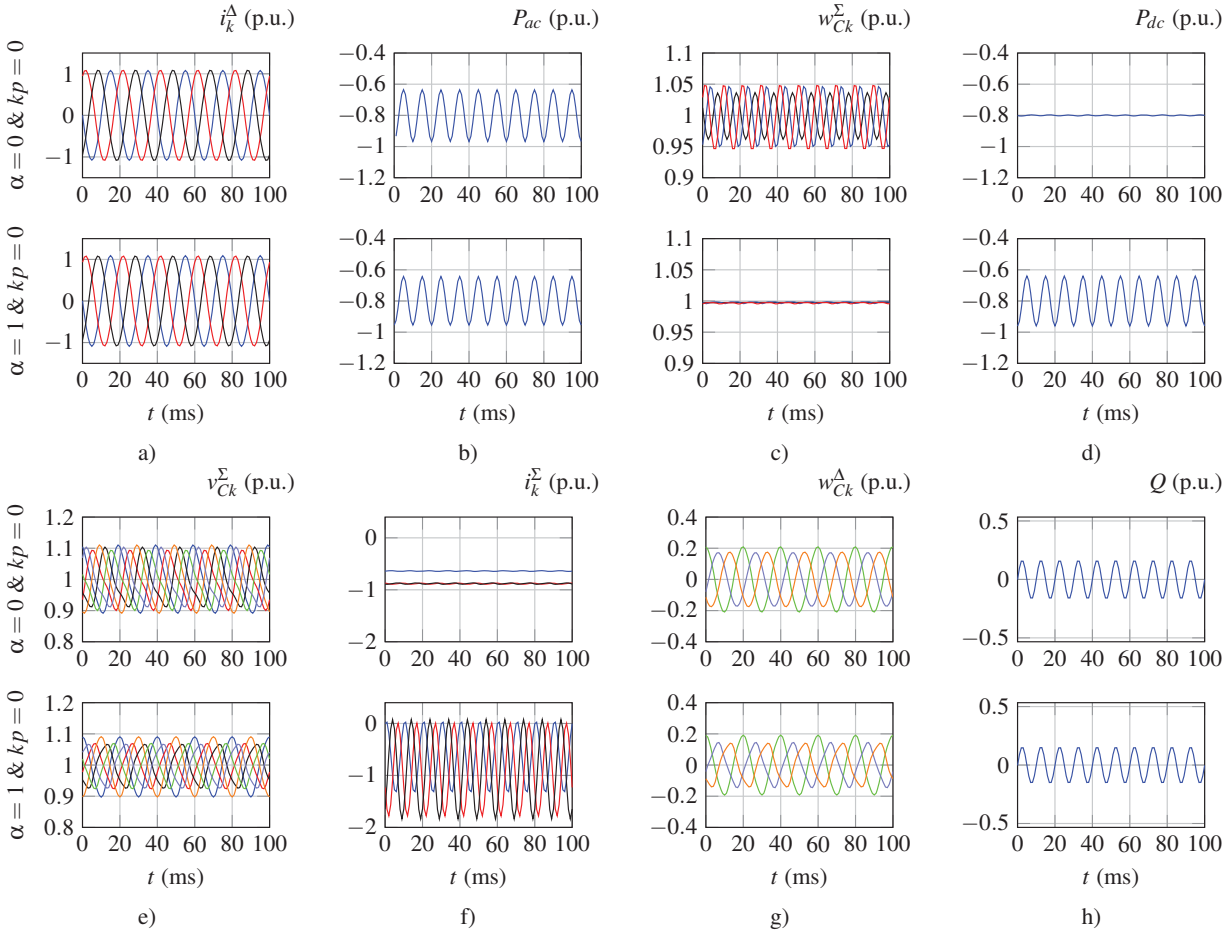

Fig. 7. MMC variables under unbalanced grid operation with circulating current references calculated by (16) [26]. a) *ac*-grid currents, b) *ac* active power, c) MMC capacitive energy sum, d) power at the *dc* terminals, e) MMC capacitor voltages, f) circulating currents, g) energy difference between arms h) reactive power.

($kp = 0$) and oscillation-free reactive power ($kp = 1$). The aim of this section is twofold. First, to validate (24) as a suitable control option for the MMC under unbalanced conditions. Second, to give insight on the performance of the MMC under unbalanced conditions with oscillation-free power at the *dc* terminals and the different *ac* grid current control strategies mentioned above. In Fig. 8, a matrix of individual figures is shown representing the MMC grid currents, the *ac*-side active power, the energy sum stored in the capacitors for each phase, and the power at the *dc* terminals; for different values of $kp \in [-1, 0, +1]$ and $\alpha \in [0, 1]$. The series of plots is continued in Fig. 9, showing the MMC capacitor voltages, the circulating currents, the energy difference between arms and the reactive power.

1) Comparison between the two circulating current reference formulations: As a first remark, notice that the instantaneous power at the *dc* terminals of the MMC controlled by (24) and depicted in Fig. 8 has a better performance in terms of the quality of the output waveform than the results depicted in Fig 7, *independently of the value of* α. This is because the constant *dc* power requirement was formulated as a strict constraint in the optimization problem, and all other requirements regarding the energy balancing are part of the objective function. Furthermore, when operating with (24) and $\alpha = 1$, the capacitive energy sum in each phase presents more oscillations than the equivalent case depicted in Fig. 7, since the buffering of power fluctuations originating from the *ac*-side is prioritized. Nonetheless, the oscillations in the stored energy are limited as much as possible.

2) The case of oscillation-free ac *-side active power with sinusoidal currents ($kp = -1$):* When $kp = -1$, neither the *ac*-side power at the PCC nor the power between the *dc* terminals present any observable oscillations. However, the stored capacitive energy sum variable has a clear zero-sequence oscillation component, which is compensating for the power fluctuations in the inductors, which are in turn caused by the unbalanced *ac*-side currents. This phenomenon is further analyzed in the following lines. By power preservation–i.e., Tellegen's theorem–the power that will enter the MMC, say P_s, can be defined as

$$P_s = R' \sum_{k \in abc} (i_k^{\Delta})^2 + \sum_{k \in abc} \dot{w}_{Lk} + P_{ac},$$

with R' being the equivalent *ac*-side resistance as seen from the MMC, and w_{Lk} representing the energy stored in the equivalent inductor L' of a single phase k. The three phase power fluctuating in the resistance and inductance can be

This article has been accepted for publication in a future issue of this journal, but has not been fully edited. Content may change prior to final publication. Citation information: DOI 10.1109/JESTPE.2019.2894677, IEEE Journal of Emerging and Selected Topics in Power Electronics

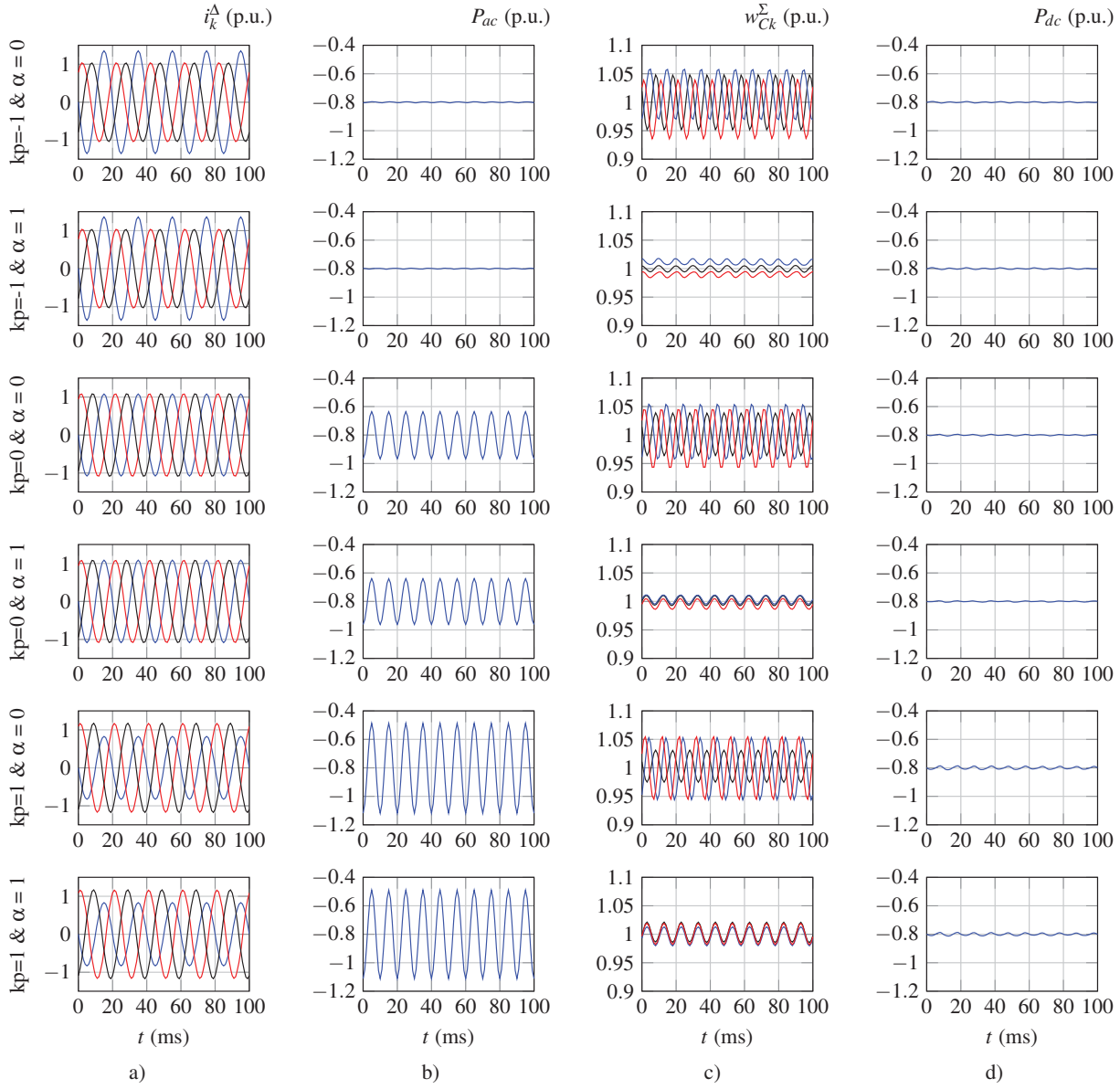

Fig. 8. Operation of MMC during unbalanced conditions with proposed control method, illustrated by the following variables: a) *ac* grid-side currents, b) *ac* grid-side active power, c) MMC capacitive phase energy sum, d) power at the MMC *dc* terminals.

easily computed as;

$$R' \sum_{k\in abc} (i_k^{\Delta})^2 = R' \left((i_a^{\Delta})^2 + (i_b^{\Delta})^2 + (i_c^{\Delta})^2 \right)$$
$$= R' \left((i_a^{\Delta+} + i_a^{\Delta-})^2 + (i_b^{\Delta+} + i_b^{\Delta-})^2 + (i_c^{\Delta+} + i_c^{\Delta-})^2 \right)$$

$$\sum_{k\in abc} \dot{w}_{Lk} = \frac{d}{dt} \frac{L' \left((i_a^{\Delta})^2 + (i_b^{\Delta})^2 + (i_c^{\Delta})^2 \right)}{2}$$
$$= L' \frac{d}{dt} \frac{\left((i_a^{\Delta+} + i_a^{\Delta-})^2 + (i_b^{\Delta+} + i_b^{\Delta-})^2 + (i_c^{\Delta+} + i_c^{\Delta-})^2 \right)}{2}$$

After some simple calculations, one can see that the the above expressions will only result in constant values in steady-state if either $i_{abc}^{\Delta-} = 0$ or $i_{abc}^{\Delta+} = 0$. Thus, the presence of a negative sequence *ac*-side current will produce power fluctuations proportional to the equivalent inductance which in turn will enter the MMC.

3) The case of balanced sinusoidal currents ($kp = 0$): When $kp = 0$ (refer to the third and fourth rows of Fig. 8 and 9 the *ac*-side currents are being controlled to be balanced by means of (25) even under the presence of the unbalanced *ac* grid voltage. The product between balanced grid currents and unbalanced *ac* grid voltages will result in a fluctuating power at the PCC at twice the grid fundamental frequency. However, using the presented strategy for circulating current control, the MMC will store such power oscillations inside its distributed capacitors, thus preventing them from appearing at the *dc* terminals. In addition, and contrary to the previous case, there is no need to compensate any additional power oscillations in the *ac* grid inductances since the grid currents are balanced.

4) The case of oscillation-free reactive power with sinusoidal currents ($kp = +1$): Comparing the fifth and sixth rows of Fig. 8 corresponding to the case of oscillation free reactive

This article has been accepted for publication in a future issue of this journal, but has not been fully edited. Content may change prior to final publication. Citation information: DOI 10.1109/JESTPE.2019.2894677, IEEE Journal of Emerging and Selected Topics in Power Electronics

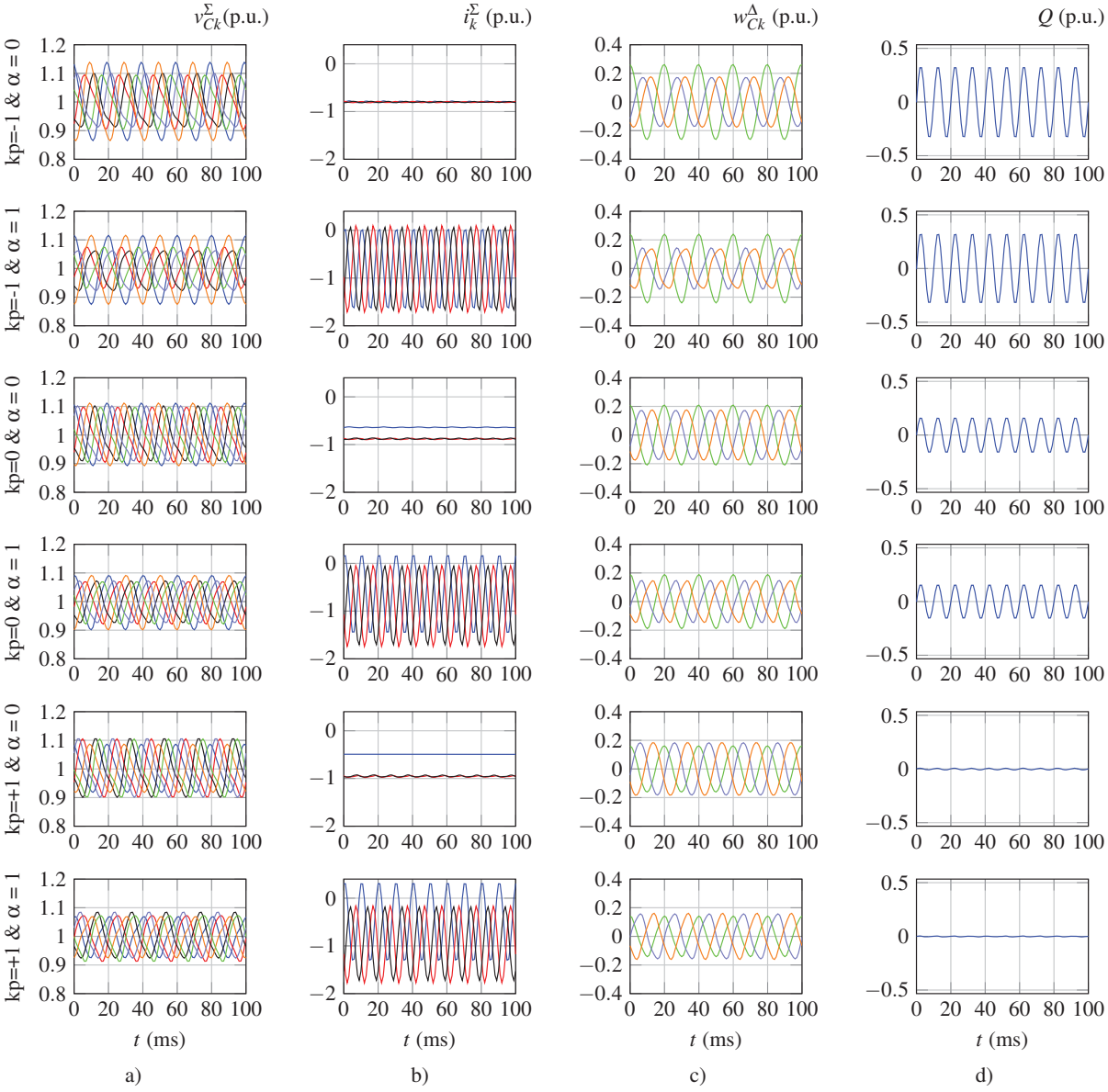

Fig. 9. Continuation of Fig. 8 with the following MMC variables during unbalanced grid operation: a) MMC capacitor voltages, b) circulating currents, c) energy difference between arms d) reactive power

power with the rest of the sub-figures, it can be seen that it is the case in which the MMC capacitive energy storing capability is required the most. More precisely, the capacitive energy in the MMC $\sum_{k\in abc} w_{Ck}^{\Sigma}$ fluctuates more than any of the other cases corresponding to $kp = 0$ and $kp = -1$. This is easier to notice when $\alpha = 1$ than when $\alpha = 0$, since for the former case the stored capacitive energy sum of each phase w_{Ck}^{Σ} are in phase with one another. This allows to clearly notice how the oscillations of the zero sequence of this variable reaches its highest value when $kp = +1$, its lowest when $kp = -1$, and an intermediate value when $kp = 0$ [7]. This is since the MMC is compensating for both energy fluctuations "sources"; i.e., 1) the inductive energy fluctuations due to the unbalanced grid currents, and 2) the fluctuating *ac*-side power, which is significantly higher than for the other cases.

By contrast, the oscillation-free reactive power control seems to be the case with the smallest energy difference oscillations between arms, which results in the case with smallest fluctuations of MMC capacitor voltages ($v_{Ck}^{U,L}$). Note that when $kp = +1$, the energy difference oscillations and the MMC capacitor voltages are much lower than for the other values of kp, especially compared to the case of $kp = -1$. Thus, ensuring constant instantaneous reactive power ($kp = +1$) during unbalances tends to reduce the voltage stress of the arm capacitors.

From the fourth column of Fig. 8, it is possible to observe some small oscillations at the *dc* power, which are fluctuating at twice the grid frequency. These oscillations are in fact introduced by $P_{\mathrm{PB}}^{\mathrm{ref}}$ in (26), through $\overline{P}_{dc}^{*}$, and are associated to the dynamics of the filtering technique used to determine $\overline{w}_{C3\phi}^{\Sigma\mathrm{ref}}$. They are also bigger for the case in which $kp = +1$,

[7] When $\alpha = 0$, the same pattern may be found by adding the three energy sums w_{Ck}^{Σ} of each phase.

This article has been accepted for publication in a future issue of this journal, but has not been fully edited. Content may change prior to final publication. Citation information: DOI 10.1109/JESTPE.2019.2894677, IEEE Journal of Emerging and Selected Topics in Power Electronics

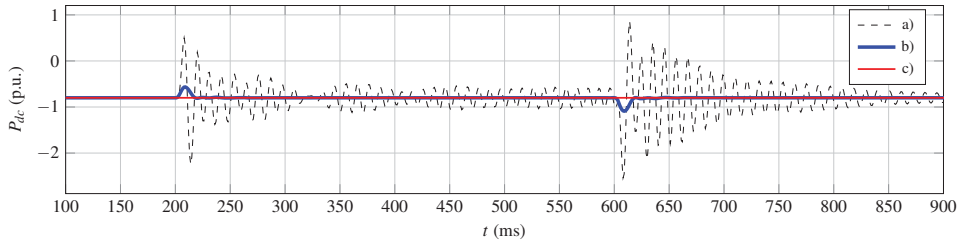

Fig. 10. Power at the *dc* terminals of the MMC facing an unbalanced grid operation between $t = 200ms$ and $t = 600ms$, under the following control schemes: a) Circulating Current Suppression Controller, b) the formulation of (23) with $P^*_{ac} = P^{ref}_{\text{OP}}$ and $P^*_{dc} = P^{ref}_{\text{PB}}$, and c) the formulation of (23) with $P^*_{dc} = P^{ref}_{\text{OP}}$ and $P^*_{ac} = P^{ref}_{\text{PB}}$.

since this is the case in which $w^{\Sigma\text{ref}}_{C3\phi}$ is the biggest, as can be inferred from the third column of the same figure. Thus, it is expected that improving the filtering technique will result in a less oscillatory *dc* power.

5) Relationship between the circulating currents, kp and the ac*-side power oscillations:* Another interesting observation can be made by analyzing the mean value of the circulating currents for each case. For $kp = -1$, there is no significant difference between the mean value of each of the phases. This is because constant 3-phase power is achieved by increasing the current in the phase with reduced voltage. Thus, the *ac*-side power control is ensuring equal average power in the three phases, which corresponds to equal *dc* component of the circulating current. Nevertheless, when $kp = 0$, the mean value of i^{Σ}_a is decreased compared to the other two phases since this case does not ensure constant power per phase, but a power proportional to the voltage at the PCC. The difference observed between the phases is the most significant when $kp = +1$, as it is also the case with highest *ac*-side power oscillations.

6) Final remarks: Working directly in *abc* coordinates in the stationary frame enables the possibility of directly regulating phase-independently the mean values of the capacitive energy sum and difference stored in the arms of the MMC (i.e.: $\overline{w}^{\Sigma}_{Ck}$ & $\overline{w}^{\Delta}_{Ck}$). Indeed, this translates into the MMC capacitor voltages having the desired average voltage value regardless of the unbalanced condition and the grid current control method used to cope with it.

The circulating current control reference of (24) will ensure that the sum of the circulating currents will be oscillation-free regardless of the value of α. Thus constant power at the *dc* terminals of the converter is ensured for every case.

If the MMC is operated with $\alpha = 1$, the capacitive energy storage capacity of the MMC ($\sum_{k\in(abc)} w^{\Sigma}_{Ck}$) will be utilized most efficiently as only the zero-sequence component will appear. This is not the case for $\alpha = 0$ since besides the zero sequence, positive and negative sequences appear as well.

The presented results show that the MMC can always be controlled to prevent steady-state power oscillations from the *ac* side from entering the *dc* grid. Thus, the MMC can be controlled to act as a *power oscillation firewall*, as long as the capacitance is designed to handle the fluctuations. Controlling the power oscillations on the *ac* side can limit the energy sum oscillations. However, the internal arm capacitor voltages–similar to the energy difference–is highly dependent on the fluctuation of the reactive power at the ac side. Thus, constant instantaneous reactive power control can minimize the MMC sub-module capacitor voltage oscillations during unbalanced operation.

C. Influence of the two active power control objectives

This section intends to show the difference between the Case A and Case B defined and discussed in section V. In Fig. 10, it is possible to notice three curves, all representing the power at the *dc* terminals of the converter under a *transient* unbalanced fault between $t = 0.2\ s$ and $t = 0.6\ s$ given by the same fault conditions as in the previous simulations. Each of the curves is obtained with a different control strategy, as follows:

a) First, the CCSC from [11] is used, only as a reference. This case has no explicit control of the zero sequence component of the circulating current (unlike [14]), and hence it is not capable of ensuring constant power.
b) As a second case, the power at the *dc* terminals of the converter resulting from applying (24) under the configuration defined as Case A in section V is presented. It can be seen how the oscillations are significantly reduced with respect to the reference case, yet it is possible to notice a small transient at $t = 0.2\ s$ and at $t = 0.6\ s$. These transients are generated by (26) through the *dc* power reference $\overline{P}^*_{dc}$.
c) Finally, the last curve depicts a signal with no noticeable transient. This result is obtained by applying (24) under the configuration defined as Case B in section V. By doing so, all the dynamical effects caused by the PI controller of (26) are now shifted to the *ac*-side of the converter, leaving the *dc* side of the MMC absolutely decoupled from any kind of disturbance within its rated operating conditions.

The rest of the variables for the event under consideration are shown in Fig. 11 for Case A, and Case B. As expected, the transitory peaks that were found in the power at the *dc* terminals of the MMC under Case A configuration have been shifted into the *ac*-side power for Case B, and are therefore absorbed by the distributed capacitive energy storage of the MMC.

VII. Conclusion

An approach for optimal shaping of the circulating currents in Modular Multilevel Converters (MMC) under unbalanced operating conditions, based on constrained mathematical optimization in *abc* coordinates by the Lagrange multipliers

This article has been accepted for publication in a future issue of this journal, but has not been fully edited. Content may change prior to final publication. Citation information: DOI 10.1109/JESTPE.2019.2894677, IEEE Journal of Emerging and Selected Topics in Power Electronics

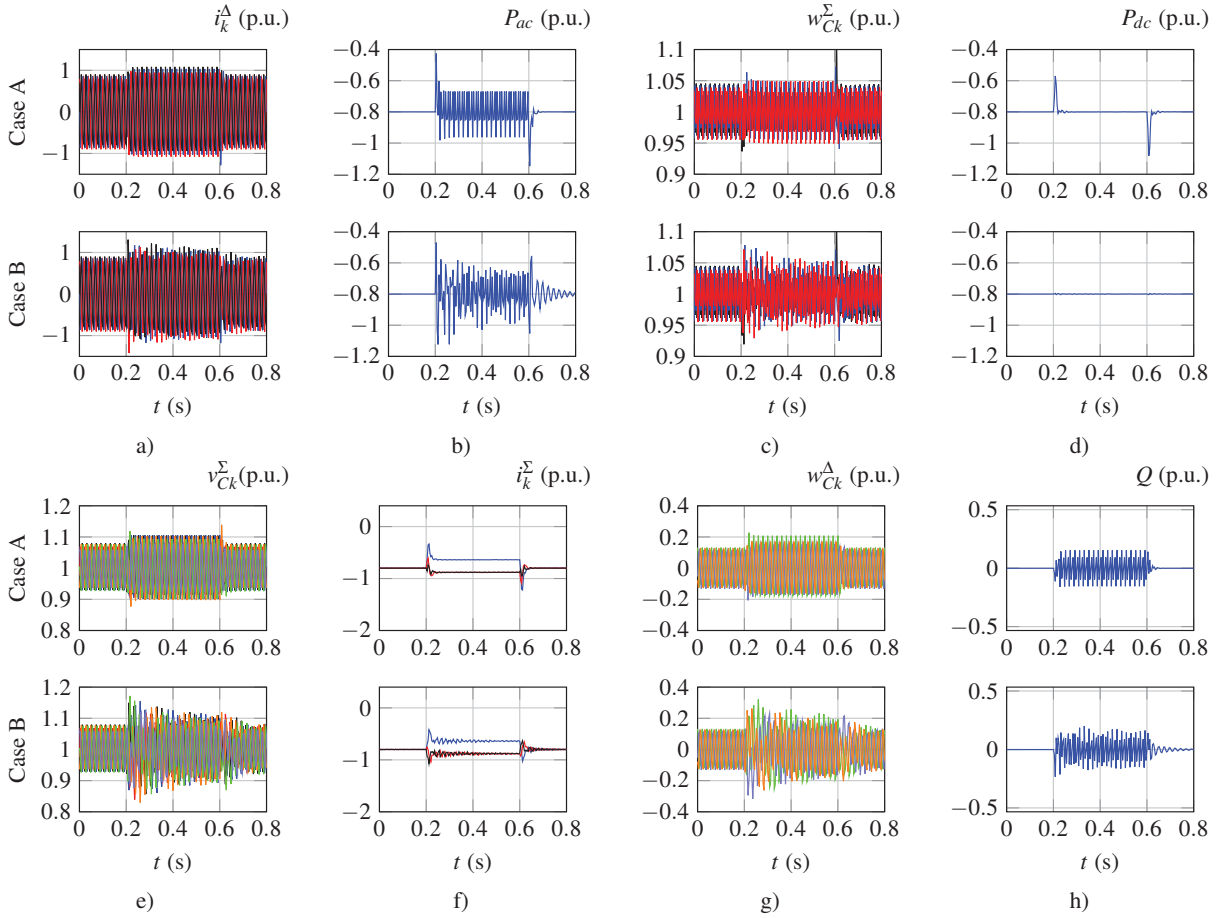

Fig. 11. MMC variables during an unbalanced grid operation between $t = 200ms$ and $t = 600ms$, with kp = 0 and α= 0. a) *ac*-grid currents, b) *ac* active power, c) MMC capacitive energy sum, d) power at the *dc* terminals, e) MMC capacitor voltages, f) circulating currents, g) energy difference between arms h) reactive power.

method, is presented and analyzed in this paper. The applied optimization procedure yields analytical expressions for the calculation of circulating current references for each phase of the MMC that will ensure constant, non-oscillatory, power flow at the *dc* side of the converter under unbalanced *ac* grid voltage conditions, independently from the power control objectives at the *ac*-side. The condition of non-oscillatory power flow at the *dc*-side of the converter can be achieved while minimizing either the oscillations of the capacitive energy sum or the circulating current per phase. In both these cases, the applied strategy for circulating current reference calculation for the MMC is capable of preventing steady state power oscillations at the *ac*-side during unbalanced conditions from propagating into the *dc* side.

Furthermore, it has been shown that by using the circulating currents instead of the *ac*-side currents to establish the constant power operating point of the MMC, both steady state and transient power fluctuations or perturbations from the *ac*-grid will be prevented from propagating to the *dc* terminals of the MMC, as long as the operation of the converter is kept within its rated conditions. Thus, the MMC can be controlled to act as a *power oscillation firewall* where the distributed capacitance of the MMC topology is utilized to effectively decouple the power flow in the *ac* and *dc* sides. Such operation of the MMC can be especially relevant for (multi-terminal) HVDC systems where unintended *dc*-side power fluctuations and thus *dc* voltage fluctuations should be avoided, since they will negatively influence other converters connected to the same *dc*-network.

For assessing the operation of the MMC under different operating conditions, three strategies for *ac*-side power control during unbalanced *ac* grid voltage conditions have been simulated with the proposed strategy for circulating current reference calculation. This analysis intends to provide insight into the operation of the MMC converter under unbalanced conditions when controlled according to the proposed approach. It was shown that, regardless of the applied *ac*-side control strategy, the internal energy storage capacity of the MMC is able to decouple the power oscillations of the *ac* side from the *dc* side. Nonetheless, each control strategy has a different effect on the internal MMC variables, as demonstrated by the presented results. This should be taken into account in the design and control of each particular application. More precisely, it was seen how controlling the MMC with constant instantaneous reactive power during the unbalanced conditions reduced the voltage oscillations in internal MMC capacitors, which can have important consequences for their required size and ratings.

REFERENCES

[1] L. Xu, B. Andersen, and P. Cartwright, "VSC transmission operating under unbalanced ac conditions - analysis and control design," *IEEE Trans. Power Del.*, vol. 20, no. 1, pp. 427–434, 2005.

[2] J. Suul, A. Luna, and P. Rodriguez, "Power control of VSC HVDC converters for limiting the influence of ac unbalanced faults on multi-terminal dc grids," in *Proc. 10th IET Int. Conf. AC and DC Power Transmiss. (ACDC)*, 2012, pp. 1–7.

[3] P. Rodriguez, A. Timbus, R. Teodorescu, M. Liserre, and F. Blaabjerg, "Flexible active power control of distributed power generation systems during grid faults," *IEEE Trans. Ind. Electron.*, vol. 54, no. 5, pp. 2583–2592, 2007.

[4] F. Wang, J. Duarte, and M. Hendrix, "Pliant active and reactive power control for grid-interactive converters under unbalanced voltage dips," *IEEE Trans. Power Electron.*, vol. 26, no. 5, pp. 1511 –1521, May 2011.

[5] R. Teodorescu, M. Liserre, and P. Rodriguez, *Grid Converters for Photovoltaic and Wind Power Systems*. Wiley-IEEE Press, 2011.

[6] C. H. Ng, L. Ran, and J. Bumby, "Unbalanced-grid-fault ride-through control for a wind turbine," *IEEE Trans. Ind. Appl.*, vol. 44, no. 3, pp. 845–856, 2008.

[7] P. Rodríguez, A. Luna, I. Candela, R. Mujal, R. Teodorescu, and F. Blaabjerg, "Multiresonant frequency-locked loop for grid synchronization of power converters under distorted grid conditions," *IEEE Trans. Ind. Electron.*, vol. 58, no. 1, pp. 127–138, 2011.

[8] A. Junyent-Ferré, O. Gomis-Bellmunt, T. C. Green, and D. E. Soto-Sanchez, "Current control reference calculation issues for the operation of renewable source grid interface vscs under unbalanced voltage sags," *IEEE Trans. Power Electron.*, vol. 26, no. 12, pp. 3744–3753, 2011.

[9] J. A. Suul, "Control of grid integrated voltage source converters under unbalanced conditions: Development of an on-line frequency-adaptive virtual flux-based approach," *PhD Dissertation, Norwegian University of Science and Technology*, 2012.

[10] A. Lesnicar and R. Marquardt, "An innovative modular multilevel converter topology suitable for a wide power range," in *Proc. IEEE Bologna Power Tech Conf.*, vol. 3, June 2003, p. 6 pp. Vol.3.

[11] Q. Tu, Z. Xu, and L. Xu, "Reduced switching-frequency modulation and circulating current suppression for modular multilevel converters," *IEEE Trans. Power Del.*, vol. 26, no. 3, pp. 2009 –2017, July 2011.

[12] G. Bergna, J. A. Suul, E. Berne, J.-C. Vannier, and M. Molinas, "MMC circulating current reference calculation in abc frame by means of Lagrange multipliers for ensuring constant dc power under unbalanced grid conditions," in *Proc. 16th Eur. Conf. Power Electron. and Appl., (EPE'14 ECCE Europe)*, 2014, pp. 1–10.

[13] J. Li, G. Konstantinou, H. R. Wickramasinghe, and J. Pou, "Operation and control methods of modular multilevel converters in unbalanced ac grids: A review," *IEEE Trans. Emerg. Sel. Topics Power Electron.*, vol. Early Access, 2018.

[14] G. Bergna, J. Suul, E. Berne, P. Egrot, P. Lefranc, J.-C. Vannier, and M. Molinas, "Mitigating dc-side power oscillations and negative sequence load currents in modular multilevel converters - First approach using resonant PI," in *Proc. IEEE Montreal IECON Conf.*, October 2012.

[15] Q. Tu, Z. Xu, Y. Chang, and G. Li, "Suppressing dc voltage ripples of MMC-HVDC under unbalanced grid conditions," *IEEE Trans. Power Del.*, vol. 27, no. 3, pp. 1332 –1338, July 2012.

[16] M. Guan and Z. Xu, "Modeling and control of a modular multilevel converter-based HVDC system under unbalanced grid conditions," *IEEE Trans. Power Electron.*, vol. 27, no. 12, pp. 4858–4867, 2012.

[17] Y. Zhou, D. Jiang, J. Guo, P. Hu, and Y. Liang, "Analysis and control of modular multilevel converters under unbalanced conditions," *IEEE Trans. Power Del.*, vol. 28, no. 4, pp. 1986–1995, 2013.

[18] A. E. Leon and S. J. Amodeo, "Energy balancing improvement of modular multilevel converters under unbalanced grid conditions," *IEEE Trans. Power Electron.*, vol. 32, no. 8, pp. 6628–6637, 2017.

[19] S. Li, Z. Yao, and Z. Peng, "Circulating current suppressing strategy for MMC-HVDC based on nonideal proportional resonant controllers under unbalanced grid conditions," *IEEE Trans. Power Electron.*, vol. 30, no. 1, pp. 387–397, 2015.

[20] J. Wang, J. Liang, C. Wang, and X. Dong, "Circulating current suppression for MMC-HVDC under unbalanced grid conditions," *IEEE Trans. Ind. Appl.*, vol. 53, no. 4, pp. 3250–3259, 2017.

[21] J. Freytes, L. Papangelis, H. Saad, P. Rault, T. V. Cutsem, and X. Guillaud, "On the modeling of MMC for use in large scale dynamic simulations," in *Proc. IEEE Power Syst. Comput. Conf. (PSCC)*, 2016, pp. 1–7.

[22] J.-W. Moon, C.-S. Kim, J.-W. Park, D.-W. Kang, and J.-M. Kim, "Circulating current control in MMC under the unbalanced voltage," *IEEE Trans. on Power Del.*, vol. 28, no. 3, pp. 1952–1959, 2013.

[23] Y. Zhou, D. Jiang, J. Guo, P. Hu, and L. Zhiyong, "Control of modular multilevel converter based on stationary frame under unbalanced ac system," in *Proc. 3rd Digit. Manuf. Autom. Conf. (ICDMA)*, 2012, pp. 293–296.

[24] M. Saeedifard and R. Iravani, "Dynamic performance of a modular multilevel back-to-back HVDC system," *IEEE Trans. Power Del.*, vol. 25, no. 4, pp. 2903–2912, 2010.

[25] Y. Liang, J. Liu, and Q. Yang, "Arm current control strategy for MMC-HVDC under unbalanced conditions," *IEEE Trans. Power Del.*, vol. 32, no. 1, pp. 125–134, 2017.

[26] G. Bergna, A. Garces, E. Berne, P. Egrot, A. Arzande, J.-C. Vannier, and M. Molinas, "A generalized power control approach in abc frame for modular multilevel converter HVDC links based on mathematical optimization," *IEEE Trans. Power Del.*, vol. 29, no. 1, pp. 386–394, Feb. 2014.

[27] G. Bergna, E. Berne, A. Garces, P. Egrot, J.-C. Vannier, and M. Molinas, "A generalized power control approach in abc frame for modular multilevel converters based on Lagrange multipliers," in *Proc. 15th Eur. Conf. Power Electron. Appl. (EPE ECCE-Europe)*, 2013, pp. 1–8.

[28] A. Garces, M. Molinas, and P. Rodriguez, "A generalized compensation theory for active filters based on mathematical optimization in abc frame," *Electr. Power Syst. Research*, vol. 90, no. 0, pp. 1 – 10, 2012.

[29] H. Akagi, M. Aredes, and E. Watanabe, *Instantaneous Power Theory and Applications to Power Conditioning*. Wiley-IEEE Press, 2007.

[30] G. Bergna, J.-A. Suul, E. Berne, P. Egrot, J.-C. Vannier, and M. Molinas, "Generalized abc frame differential current control ensuring constant dc power for modular multilevel converters under unbalanced operation," in *Proc. 15th Eur. Conf. Power Electron. Appl. (EPE-ECCE Europe)*, 2013, pp. 1–10.

[31] G. Bergna, J. A. Suul, E. Berne, P. Egrot, J.-C. Vannier, and M. Molinas, "Analysis of modular multilevel converters under unbalanced grid conditions with different load current control strategies and Lagrange-based differential current control," in *Proc. 1st Int. Future Energy Electron. Conf. (IFEEC)*, 2013, pp. 669–674.

[32] G. Bergna-Diaz, "Modular multilevel converter control for HVDC operation: Optimal shaping of the circulating current signal for internal energy regulation," Ph.D. dissertation, École CentraleSupélec and The Norwegian University of Science and Technology, 2015.

[33] L. Harnefors, A. Antonopoulos, S. Norrga, L. Angquist, and H. Nee, "Dynamic analysis of modular multilevel converters," *IEEE Trans. Ind. Electron.*, vol. 60, no. 7, pp. 2526–2537, July 2013.

[34] H. Saad, X. Guillaud, J. Mahseredjian, S. Dennetire, and S. Nguefeu, "MMC capacitor voltage decoupling and balancing controls," *IEEE Trans. Power Del.*, vol. 30, no. 2, pp. 704–712, April 2015.

[35] A. Antonopoulos, L. Angquist, and H.-P. Nee, "On dynamics and voltage control of the modular multilevel converter," in *Proc. 13th Eur. Conf. Power Electron. Appl. (EPE-ECCE Europe)*, sept. 2009, pp. 1 –10.

[36] X. Yuan, W. Merk, H. Stemmler, and J. Allmeling, "Stationary-frame generalized integrators for current control of active power filters with zero steady-state error for current harmonics of concern under unbalanced and distorted operating conditions," *IEEE Trans. Ind. Appl.*, vol. 38, no. 2, pp. 523–532, Mar 2002.

[37] A. de Heredia, H. Gaztanaga, I. Etxeberria-Otadui, S. Bacha, and X. Guillaud, "Analysis of multi-resonant current control structures and tuning methods," in *Proc. IEEE 32nd Conf. Ind. Electron. (IECON)*, Nov. 2006, pp. 2156–2161.

[38] F. J. Rodriguez, E. Bueno, M. Aredes, L. G. B. Rolim, F. A. S. Neves, and M. C. Cavalcanti, "Discrete-time implementation of second order generalized integrators for grid converters," in *Proc. IEEE 34th Conf. Ind. Electron. (IECON)*, 2008, pp. 176–181.

[39] P. Rodriguez, G. Medeiros, A. Luna, M. C. Cavalcanti, and R. Teodorescu, "Safe current injection strategies for a STATCOM under asymmetrical grid faults," in *Proc. IEEE Energy Convers. Congr. Expo. (ECCE)*, 2010, pp. 3929–3935.

[40] P. Rodriguez, A. Luna, R. Muñoz Aguilar, I. Etxeberria-Otadui, R. Teodorescu, and F. Blaabjerg, "A stationary reference frame grid synchronization system for three-phase grid-connected power converters under adverse grid conditions," *IEEE Trans. Power Electron.*, vol. 27, no. 1, pp. 99–112, 2012.

[41] G. Bergna, J. A. Suul, and S. S. D'Arco, "Impact on small-signal dynamics of using circulating currents instead of ac-currents to control the dc voltage in MMC HVDC terminals," in *Proc. IEEE Energy Convers. Congr. Expo. (ECCE)*, 2016, pp. 1–8.

This article has been accepted for publication in a future issue of this journal, but has not been fully edited. Content may change prior to final publication. Citation information: DOI 10.1109/JESTPE.2019.2894677, IEEE Journal of Emerging and Selected Topics in Power Electronics

[42] J. Zhu, C. D. Booth, G. P. Adam, A. J. Roscoe, and C. G. Bright, "Inertia emulation control strategy for VSC-HVDC transmission systems," *IEEE Trans. Power Syst.*, vol. 28, no. 2, pp. 1277–1287, 2013.
[43] S. D'Arco, G. Guidi, and J. A. Suul, "Operation of a modular multilevel converter controlled as a virtual synchronous machine," in *Proc. Int. Power Electron. Conf. IEEE IPEC Niigata - ECCE Asia*, 2018, pp. 782–789.
[44] J. Peralta, H. Saad, S. Dennetiere, J. Mahseredjian, and S. Nguefeu, "Detailed and averaged models for a 401-level MMC HVDC system," *IEEE Trans. Power Del.*, vol. 27, no. 3, pp. 1501 –1508, July 2012.
[45] G. Bergna, J. Suul, A. Garces, E. Berne, P. Egrot, A. Arzande, J.-C. Vannier, and M. Molinas, "Improving the dynamics of Lagrange-based MMC controllers by means of adaptive filters for single-phase voltage, power and energy estimation," in *Proc. IEEE 39th Ind. Electron. Conf. (IECON)*, Nov 2013, pp. 6239–6244.
[46] S. Rohner, J. Weber, and S. Bernet, "Continuous model of modular multilevel converter with experimental verification," in *Proc. IEEE Energy Convers. Congr. Expo. (ECCE)*, 2011, pp. 4021–4028.
[47] W. Yang, Q. Song, and W. Liu, "Decoupled control of modular multilevel converter based on intermediate controllable voltages," *IEEE Trans. Ind. Electron.*, vol. 63, no. 8, pp. 4695–4706, 2016.

Gilbert Bergna-Diaz (M'19) received the electrical power engineering degree from the Universidad Simón Bolívar, Caracas, Venezuela, in 2008, the Research Master degree in electrical energy from the École Supérieure d'Électricité (Supélec), Paris, France, in 2010, and the joint Ph.D. degree in electric power engineering from École CentraleSupélec, Paris, and the Norwegian University of Science and Technology (NTNU), Trondheim, Norway, in 2015.

In 2014, he joined SINTEF Energy Research as a Research Scientist, where he was involved in modelling, analysis, and control of HVDC transmission systems. Since 2016, he has been a Post-Doctoral Research Fellow at NTNU, where he is involved in energy-based modelling and nonlinear control of multi-terminal HVDC grids.

Jon Are Suul (M'11) received the M.Sc. degree in energy and environmental engineering and the Ph.D. degree in electric power engineering from the Norwegian University of Science and Technology (NTNU), Trondheim, Norway, in 2006 and 2012, respectively. From 2006 to 2007, he was with SINTEF Energy Research, Trondheim, where he was working with simulation of power electronic converters and marine propulsion systems until starting his PhD studies. From 2012, he resumed a position as a Research Scientist at SINTEF Energy Research, first in part-time position while also working as a part-time postdoctoral researcher at the Department of Electric Power Engineering of NTNU until 2016. Since August 2017, he is also serving as Adjunct Associate Professor at the Department of Engineering Cybernetic of NTNU. His research interests are mainly related to modelling, analysis and control of power electronic converters in power systems, renewable energy applications and for electrification of transport.

Erik Berne received the M.Sc. degree in Power Systems Engineering from the University College of London, United Kingdom, and from Supélec, Paris, France, in 2009. In 2009, he joined EDF R&D's Laboratory of Electrical Equipment, as a Research Engineer in Power Electronics and HVDC equipment. Since 2016, he has joined the Power System and Transmission Engineering Center (CIST) of EDF, where he is now involved in HVAC substation and HVDC system project development and execution. His research interests include power electronic converters, HV equipment and converter control aspects for grid integration of HVDC transmission.

Jean-Claude Vannier received the degree in electrical engineering from Supélec, Gif-sur-Yvette, France, in 1978, and the HDR (Accreditation to Supervise Research) degree from the Université of Paris-Sud, Orsay, France, in 2006. He is a Professor and the Head of the Department of Energy and Power Systems at CentraleSupélec, Gif-sur-Yvette, Paris-Saclay University campus, France.

He is currently conducting his researches in the field of energy conversion systems (motors, actuators and generators), with on board power grid issues. His activities range from the design to the optimal sizing, including the modelling and the control of these systems for specific applications. He has supervised 20 PhD thesis and is author of 11 patents.

Marta Molinas (M'94) received the Diploma degree in Electromechanical Engineering from the National University of Asuncion, Paraguay, in 1992; the Master of Engineering degree from Ryukyu University, Japan, in 1997; and the Doctor of Engineering degree from the Tokyo Institute of Technology, Japan, in 2000.

She was a Guest Researcher with the University of Padova, Italy, during 1998 and a JSPS Fellow in Japan from 2008 to 2009. She was a Postdoctoral Researcher (2004-2007) and Professor (2008-2014) at the Department of Electric Power Engineering, Norwegian University of Science and Technology (NTNU). She is currently Professor at the Department of Engineering Cybernetics, NTNU. Her research interests include stability of power electronics systems, harmonics, instantaneous frequency, and non-stationary signals from the human and the machine.

Prof. Molinas serves as Editor for the IEEE JOURNAL OF EMERGING AND SELECTED TOPICS IN POWER ELECTRONICS and the IEEE TRANSACTIONS ON ENERGY CONVERSION, and is an Associate Editor for the IEEE TRANSACTIONS ON POWER ELECTRONICS and the IEEE TRANSACTIONS ON INDUSTRIAL ELECTRONICS.